Appl. Phys. B (2016) 122:165
DOI 10.1007/s00340-016-6438-4

Applied Physics B
Lasers and Optics

Modulation of a double-line frequency up-conversion process in cesium vapor

Baodong Gai[1,2] · Rui Cao[1] · Xusheng Xia[1,2] · Shu Hu[1] · Jinbo Liu[1] · Jingwei Guo[1] · Yannan Tan[1] · Wanfa Liu[1] · Yuqi Jin[1] · Fengting Sang[1]

Received: 10 November 2015 / Accepted: 9 May 2016 / Published online: 28 May 2016

Abstract We have observed frequency up-conversion in Cs vapor. The pulsed pumping laser beam of 767.2 nm was converted to simultaneous collinear ultraviolet and blue radiation of wavelengths 387.7 and 455.6 nm, respectively (double-line frequency up-conversion). We examined properties of this up-conversion such as energy efficiency and pulse widths. An infrared laser of ~2.4 μm was successful in modulating the laser beam of the frequency up-conversion. The modulation shifts the wavelength of the blue radiation and the intensities of both the blue and ultraviolet radiation. At nanosecond grade, such modulations are expected to have applications in near-infrared up-conversion and optical communications.

1 Introduction

Because their beam wavelengths are short, lasers in the blue band of the visual spectra have great potential applications in under-water laser communications within the "water transmission window" [1] and information storage (such as CDs [2], compared with infrared laser). Recently, for their high efficiency and high power density, the diode pumped alkali laser (DPAL) has become a popular topic of high-power laser research. [3] To obtain extended wavelength ranges in alkali–metal vapors, generating up-conversion blue beams with laser-like properties in an alkali–metal vapor using a pumping system similar to DPAL is attracting increasing interest. In 2001, Zibrov et al. [4] reported a cw 420-nm beam from Rb vapor with a dual-wavelength pumping beam (780 and 776 nm); since then, higher conversion efficiency has been pursued by researchers. Meijer et al. [5] and Sell et al. [6] also reported 420-nm collimated radiation from the same system. Vernier et al. [7] reported a 1.1-mW 420-nm collimated radiation based on Rb vapor with a power conversion efficiency of 2.6 %. The same group also performed a study of laser transfer of orbital angular momentum using the same pumping route [8]. Sulham et al. [9] reported achieving 420-nm output with Rb vapor with a single-wavelength pulsed laser at 778 nm; a slope efficiency of 0.5 % was also achieved. For Cs vapor, Schultz et al. [10] reported a 455-nm collimated radiation output by pumping with a dual-wavelength beam (852 and 917 nm). However, from previous work, the choices of generated wavelengths for applications are few and the conversion efficiency still needs improvement. Moreover, schemes for frequency up-conversion have not been fully explored.

A nanosecond-pulsed dye laser is more convenient than any cw diode lasers for studying the transient properties of frequency up-conversion. Alkali–metal vapors have narrower absorption lines (1-GHz grade, Doppler broadened) than the usual linewidths of nanosecond-pulsed dye lasers (>3 GHz). However, the large power density (~MW/cm^2) of the pulsed dye lasers can compensate the mismatch between the narrow alkali–metal lines and the broad dye laser lines. Therefore, using nanosecond-pulsed dye lasers instead of the widely used kHz-grade narrow band cw diode lasers can realize frequency up-conversions in alkali vapor. In our experiment, nanosecond-pulsed lasers were used to produce frequency up-conversion in Cs vapor. Two new wavelengths (387.7, 455.6 nm) were identified from the

✉ Jingwei Guo
jingweiguo@dicp.ac.cn

[1] Key Laboratory of Chemical Lasers, Dalian Institute of Chemical Physics, Chinese Academy of Sciences, Dalian 116023, China

[2] University of Chinese Academy of Sciences, Beijing 100049, China

output-collimated beam. After measuring the wavelengths of the pumping laser and the generated new radiations, the states $6^2S_{1/2}$, $7^2D_{5/2}$, $7^2P_{3/2}$, and $8^2P_{3/2}$ of the Cs atom were identified with the transitions. Modulation of the frequency up-conversion using an infrared laser with wavelength of 2.42 μm (resonance transition $7^2D_{5/2} \rightarrow 7^2P_{3/2}$) was also realized. Results show that the infrared laser was successful in controlling the wavelength and pulse energy of the up-conversion. Theoretical analysis of this up-conversion and the modulation mechanism were also performed. We developed a two-step theory to explain both, including the generation of amplified spontaneous emission (ASE) and the subsequent application of four-wave mixing (FWM).

2 Experimental setup

2.1 Conversion medium

Figure 1 illustrates schematically the experimental layout. A quartz cell was filled with metal Cs vapor under vacuum. The residual background pressure of the cell at room temperature is <0.01 Pa. The inner cavity of the cell is cylindrical with a diameter of 2.5 cm and a length of 10 cm. The cell was placed in a thermostatic oven for heating during which the metal Cs vaporizes and later used as medium for the frequency up-conversion.

2.2 Frequency up-conversion

A Nd:YAG laser (GCR200, Spectra Physics, Santa Clara, CA, USA) pumped dye laser (ND6000, Continuum, San Jose, CA, USA) is used as a pump laser in this experiment. The full width at half maximum (FWHM) pulse width of the dye laser is ~2.5 ns, and the linewidth is 0.1 cm^{-1}. The repetition rate is 10 Hz. Following careful wavelength scanning of the pumping laser, an intense frequency up-conversion was found at 767.2 nm. In this work, the conversion based on a 767.2-nm pumping laser was fully examined. The ratio of the pulse energies of the generated beams and the pump beam determines the conversion efficiency. An iris with a fixed diameter of 1.5 mm placed in front of the Cs cell confined the laser beam diameter. This produced a near flattop spot intensity distribution across the beam that was then used throughout the experimental work. The pulse energies of the pumping laser and the frequency up-conversion beams were measured with an energy detector (QE12SP-S-MT-D0, Gentec-EO, Quebec City, Canada) and a photodetector (PE10B-Si-D0/DA, Gentec-EO). The pulse shape was measured using a high-speed diode detector with a bandwidth larger than 1 GHz. The spectra of the generated lasers were recorded using a spectrometer with charge-coupled device (CCD) (SynerJY iHR320, HORIBA, Kyoto, Japan).

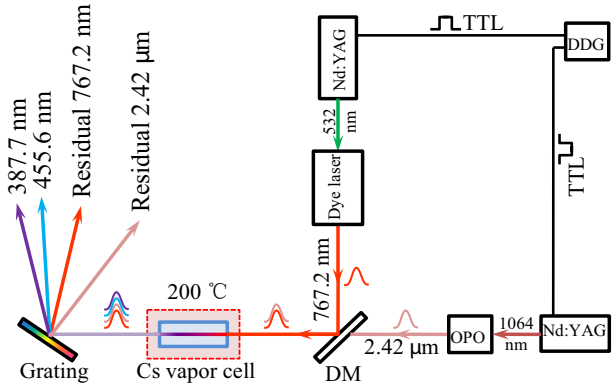

Fig. 1 Schematic of the experimental layout. A Cs vapor cell is heated to 200 °C to generate a Cs atom density of 1×10^{15} cm^{-3}. An optically pumped dye laser and an optically pumped optical parameter oscillator provide nanosecond laser pulses at ~767.2 nm and ~2.4 μm, respectively. The two beams are combined by a dichroic mirror (DM) and pass through a Cs vapor cell. A digital delay generator is used to synchronize the two lasers. Frequency up-conversion occurs in the vapor cell; a grating separates the generated radiations

2.3 Modulation

Modulation is a means of controlling the wavelength, the intensity, or other properties of a laser in real time. Because the frequency up-conversion involves specific energy levels of Cs, it is possible to modulate the conversion using transitions between these levels. A tunable infrared laser generated by an optical parameter oscillator (OPO) modulated the frequency up-conversion. A dichroic mirror was used to combine the beams from the pumping laser and the modulation laser. The OPO beam is confined to a diameter of 1.5 mm by the iris before the Cs cell to obtain a near flattop spot intensity distribution. This confined beam was used throughout the experiments. The FWHM pulse width is ~2.5 ns, and the linewidth is 0.2 cm^{-1}. The repetition rate is 10 Hz. A digital delay generator (DDG; DG645, Stanford Research Systems, Sunnyvale, CA, USA) synchronizes the dye laser and the OPO through precisely arranged TTL signals.

3 Results and discussion

3.1 Generation of blue and ultraviolet radiations

After scanning the cell temperature and the pumping wavelength, frequency up-conversion develops at a temperature of 200 °C and wavelength of 767.20 ± 0.05 nm. After passing through the cell, the pumping laser beam appears pink. A grating separates the beam into its different wavelengths,

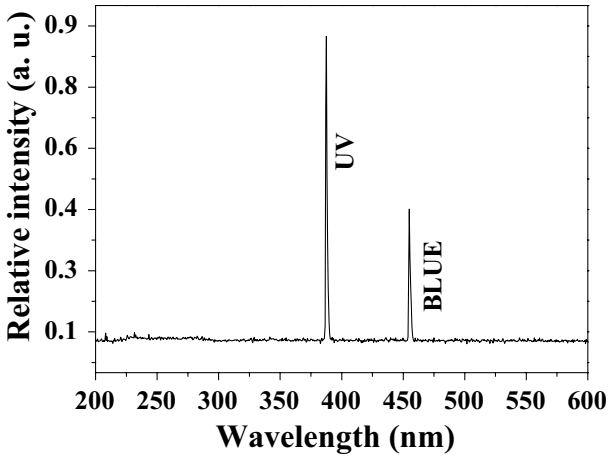

Fig. 2 Measured frequency up-conversion spectrum. The output-collimated radiations are centered at 387.7 nm (denoted as UV) and 455.6 nm (denoted as BLUE)

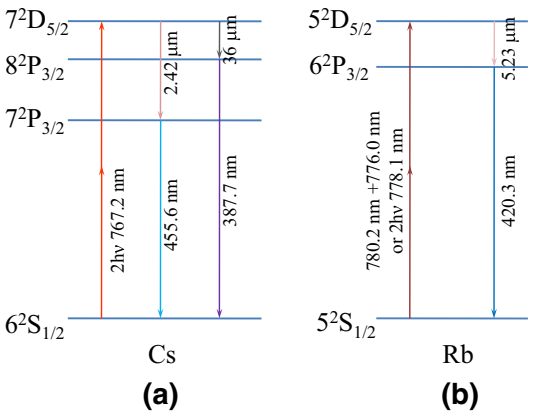

Fig. 3 **a** Schematic of four-wave mixing in Cs vapor by non-resonant one-color two-photon excitation. The wavelength of the pump laser is centered on 767.2 nm, the generated radiation is on 455.6 and 387.7 nm, and a modulation laser of 2.42 μm is used. The 36-μm radiation is inferred from the detected radiation, but has not been detected. **b** A similar process in Rb vapor is given for comparison

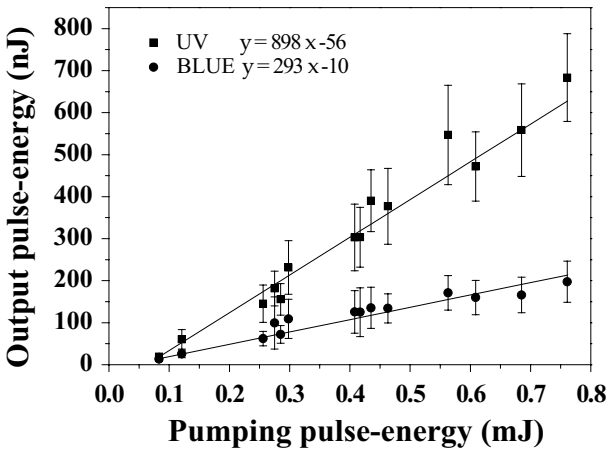

Fig. 4 Intensities of UV and BLUE recorded using a spectrometer. The conversion efficiencies are nearly constant. By measuring the same beam with energy of ~100 nJ using both the spectrometer and the nJ-grade energy detector, the spectrometer is then calibrated for measuring pulse energies. The absolute error bounds of the nJ-grade energy detector is ±30 % (not shown in the figure)

producing an ultraviolet spot and a blue spot that are clearly visible on a laser view card. Both are forward propagating and align with the pumping laser, i.e., no backward waves are observed. Moreover, both beams have the same linear polarization as that of the pumping laser. The ultraviolet radiation has a similar divergence angle to the pumping laser, whereas the blue radiation has a slightly larger divergence angle.

The output spectrum of the frequency up-conversion process (Fig. 2) shows the 387.7 and 455.6-nm peaks corresponding to the ultraviolet and blue spots, respectively; for convenience, these beams are referred to as "UV" and "BLUE," respectively. These wavelengths correlate with transitions $8^2P_{3/2} \rightarrow 6^2S_{1/2}$ ("UV") and $7^2P_{3/2} \rightarrow 6^2S_{1/2}$ ("BLUE").

An energy level scheme for these Cs transitions is depicted in Fig. 3a. Radiations at 2.42 μm and 36 μm are related to transitions $7^2D_{5/2} \rightarrow 7^2P_{3/2}$ and $7^2D_{5/2} \rightarrow 8^2P_{3/2}$, respectively, but they could not be detected because of experimental limitations. For convenience in comparison and understanding, a similar scheme for well-studied up-conversion in Rb vapor is given (Fig. 3b) [4–8].

The output energies of UV and BLUE versus pulse energy of pumping laser (Fig. 4) show that the conversion is clearly linear yielding a steady slope efficiency and a threshold pump power (<0.1 mJ/pulse for both UV and BLUE). This phenomenon is very similar to that of many ordinary laser systems when the pump power is far below saturation. The energy conversion efficiencies of the UV and BLUE are 0.08 and 0.03 %, respectively. The absorption of the pumping laser beam is too small to be detected (estimated to be <3 %).

Pulse shapes for the UV and BLUE radiation and the pumping laser beam (Fig. 5) were measured with a high-speed detector fixed in place. Switching the different beams for measurement was done by rotating the grating (Fig. 1). The arrival times of the three different pulses are comparable. To eliminate time jitter, all pulse curves were the average of a sufficient number of pulses. The arrival times for the UV, BLUE, and pumping laser pulses are almost identical, which means UV and BLUE are generated almost simultaneously following beam illumination of the Cs vapor. Of the two beams, BLUE is weaker in intensity than the UV.

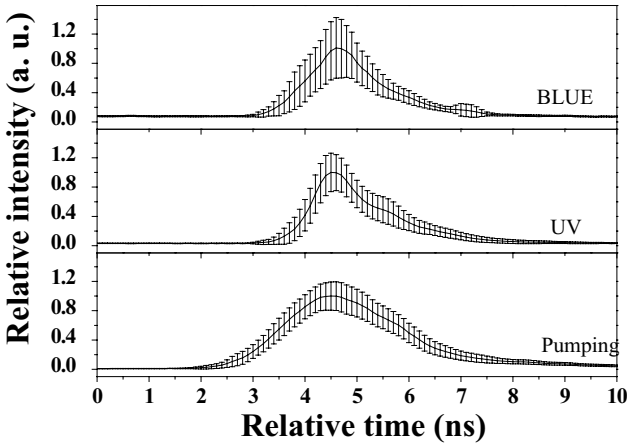

Fig. 5 Pulse shapes of the pumping laser, BLUE, and UV beams with the same reference start point. A high-speed diode detector with a rise and fall time of less than 1 ns is used for recording. Each pulse shape is an average of 100 pulses to reduce the jitter and instability as much as possible. The relative intensities of all curves are normalized

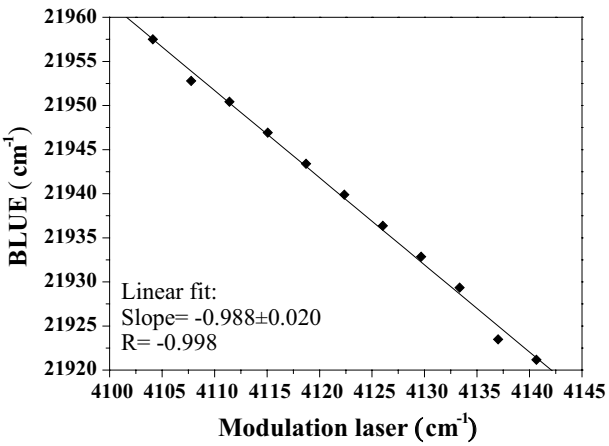

Fig. 6 Effect of the modulation laser on the frequency of the BLUE radiation. The linear fit indicates that the modulation laser and BLUE radiation exhibits a direct negative frequency correlation. The FWHM width of the measured spectral peaks (not given here) is ~5 cm^{-1}

3.2 Modulation

A laser beam of wavelength 2.42 μm is chosen to modulate the frequency up-conversion, using the transition $7^2D_{5/2} \rightarrow 7^2P_{3/2}$ (Fig. 3). In the experiment, when the beams from the pumping laser and the modulation laser are collinear and time-overlapped (illuminating the Cs vapor simultaneously), an enhancement of the BLUE spot and an attenuation of the UV spot are obvious. This result indicates a successful modulation, for which both UV and BLUE have similar divergence angle to the pumping laser.

The frequency shift of the BLUE beam is observed when the frequency of the modulating laser is tuned around 2.42 μm. A plot (Fig. 6) of the central frequencies of the BLUE spectra versus the modulation laser frequency (in cm^{-1}) shows a linear fit indicating an identical frequency displacement of the BLUE and modulation beams, but in opposite directions. The phenomenon is subject to condition

$$\nu_4 = \nu_1 + \nu_1 - \nu_3 \quad (1)$$

where ν_4, ν_1, and ν_3 are the frequencies of the BLUE, pump, and modulation laser beams, respectively.

The intensity modulations of the UV and BLUE beams by the 2.42-μm laser (Fig. 7) show a clear inverse relationship between the two normalized intensity. Without modulation, UV is stronger than BLUE. With modulation, UV is suppressed to the detection limit, and BLUE is greatly enhanced. Absolute beam energies are also compared; UV is

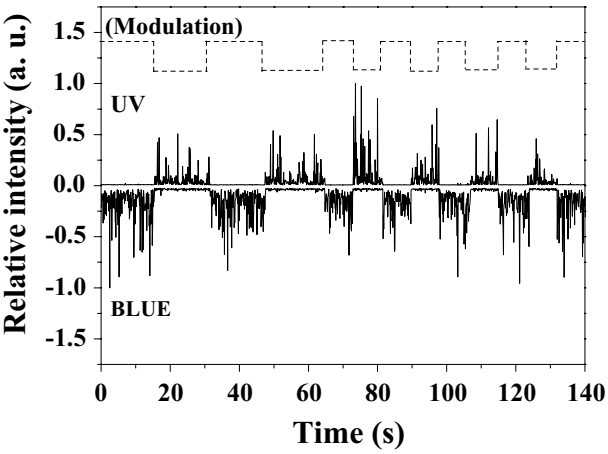

Fig. 7 Effect of the modulation on the normalized relative intensities of BLUE and UV radiation measured using two photodiodes. The energy of the 767.2-nm laser is fixed to ~0.5 mJ/pulse, and that of the modulation laser is ~0.1 mJ/pulse. The *dashed line* shows the duty cycle of the modulation laser (high for on and low for off). The UV and BLUE intensities are shown as positive and negative, respectively; the modulation is clearly observed

stronger than BLUE without modulation (Fig. 4). However, with modulation of ~ 0.1 mJ/pulse, BLUE is stronger than both the modulated UV and the original unmodulated UV.

For better understanding of the modulation process, the pulse shapes for the modulated UV and BLUE are plotted. Whereas UV is delayed by 1.4 ns (Fig. 8), BLUE does not show any obvious delay or advance and therefore is not shown here.

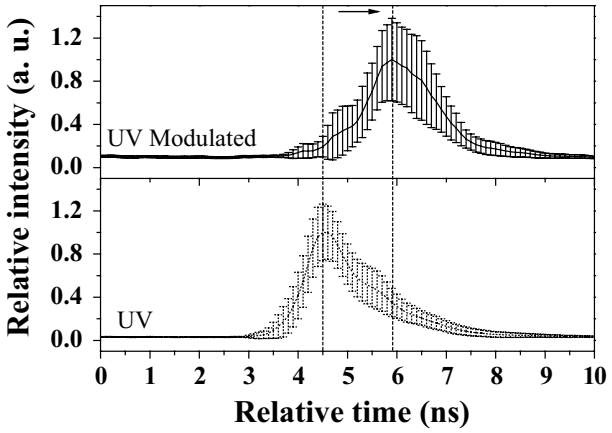

Fig. 8 Time shift of the UV pulse when the frequency up-conversion is modulated ("UV Modulated"). The curve is obtained using the same method and optical path used for Fig. 5. The UV curve in Fig. 5 is given as a *dotted line* for comparison. The shift is approximately 1.4 ns. The intensity of UV decreases considerably, as shown in Fig. 7. (Both curves are normalized for ease in viewing the figure.) Here, the energy of the 767.2-nm laser is fixed at ~0.5 mJ/pulse, and the energy of the modulation laser is ~0.1 mJ/pulse

3.3 Theoretical analysis

3.3.1 ASE and FWM

The mechanism of frequency up-conversions in previous work has not been clarified fully. The most deeply studied process is converting a dual-wavelength beam (780 and 776 nm) to 420 nm. The most popular mechanism is amplified spontaneous emission (ASE) and four-wave mixing (FWM) [5, 11], which involves two transitions and an energy criterion:

$$Rb\left(5^2S_{1/2}\right) \xrightarrow{780.2\text{ nm}+776.0\text{ nm}} Rb\left(5^2D_{5/2}\right) \tag{2}$$

$$Rb\left(5^2D_{5/2}\right) \xrightarrow{5.23\mu\text{m(ASE)}} Rb\left(6^2P_{3/2}\right) \tag{3}$$

$$h\nu_{780.2\text{ nm}} + h\nu_{776.0\text{ nm}} - h\nu_{5.23\ \mu\text{m}} \xrightarrow{\text{FWM}} h\nu_{420.3\text{ nm}} \tag{4}$$

Understanding the transitions is easiest when referring to the energy level diagram (Fig. 3b). Here transition (2) is realized through a two-photon absorption. Two photons (780.2 and 776.0 nm) are resonantly absorbed by the same Rb atom, which is excited from the $5^2S_{1/2}$ state to the $5^2D_{5/2}$ state via the $5^2P_{3/2}$ state.

Following transition (2), there are a large number of Rb atoms populated in the $5^2D_{5/2}$ state, but the lower $6^2P_{3/2}$ state is empty. Therefore, a population inversion is formed between the $5^2D_{5/2}$ and $6^2P_{3/2}$ states, which results in a stimulated emission beam at the wavelength corresponding to the ASE transition $5^2D_{5/2} \rightarrow 6^2P_{3/2}$ (5.23 μm).

FWM (4) is the last step in realizing frequency up-conversion. FWM is a parametric third-order nonlinear optics process. In a FWM process, three light waves interact in a nonlinear medium to generate a fourth light wave. In Eq. (4), the 780.2-nm beam (exciting the transition $5^2S_{1/2} \rightarrow 5^2P_{3/2}$), the 776.0-nm beam ($5^2P_{3/2} \rightarrow 5^2D_{5/2}$), and the 5.23 μm ASE beam ($5^2D_{5/2} \rightarrow 6^2P_{3/2}$) interact with Rb atoms to initiate the FWM process. The result is the absorption of the 780.2-nm beam and the 776.0-nm beam, the gain of the 5.23-μm ASE beam, and the emission of the 420.3-nm blue beam ($6^2P_{3/2} \rightarrow 5^2S_{1/2}$). From previous work, we infer that the mechanism for the up-conversion in Cs vapor is

$$2\ h\nu_{767.2\text{ nm}} - 1\ h\nu_{2.42\ \mu\text{m}} \xrightarrow{\text{FWM}} 1\ h\nu_{455.6\text{nm}} \tag{5}$$

$$2\ h\nu_{767.2\text{ nm}} - 1\ h\nu_{36\mu\text{m}} \xrightarrow{\text{FWM}} 1\ h\nu_{387.7\text{nm}} \tag{6}$$

The energy level diagram (Fig. 3a) is given for ease in understanding. First, each Cs atom can absorb two 767.2-nm photons and transitions from state $6^2S_{1/2}$ to state $7^2D_{5/2}$. Second, two ASE beams at 2.42 μm ($7^2D_{5/2} \rightarrow 7^2P_{3/2}$) and 36 μm ($7^2D_{5/2} \rightarrow 8^2P_{3/2}$) are generated. A previous study of similar transitions for Cs vapor was performed using a ruby laser [12]. Finally, the two FWM processes, Eqs. (5) and (6), occur, each FWM process comprises the interaction of two degenerate photons of 767.2 nm and one ASE photon of 2.42 μm (or 36 μm) to generate one photon of 455.6 nm (or 387.7 nm).

In a FWM process, the direction of the generated beam (light wave) is related to the three interacting beams (light waves). Conservation of the photon momenta governs this relationship. The FWMs described by Eqs. (5) and (6) should have approximately the same direction of light wave propagating directions according to photon–momenta conservation. Therefore, the convincing evidence that FWM is occurring in the conversion is that UV and BLUE are only forward propagating along with the pumping laser beam (no backward waves are observed). Being a parametric optical process, a FWM process always gives a real-time light wave conversion. Hence, the real-time characteristics of the UV and the BLUE (Fig. 5) show no absence of conformity with a FWM process.

Furthermore, the modulation is an alternative method of probing the mechanism for frequency up-conversion. From Fig. 6, Eq. (1) obtains and infers that the wavelength of the BLUE beam is determined by two wavelengths, that of the pumping laser and the modulation laser. The dual-wavelength dependence is quite consistent with FWM.

3.3.2 Mechanism of modulation

Radiation of wavelength 2.42 and 36 μm is presumed to exist and originate from ASE because of the population inversion that occurs between the $7^2D_{5/2}$ and $8^2P_{3/2}$ states, and between the $7^2D_{5/2}$ and $7^2P_{3/2}$ states. The modulation can be important evidence of the existence of ASE.

In a laser system, lasing occurs only after a population inversion has formed between two energy levels for laser transition. A small-signal gain factor G expresses the ease with which a system lases. The G factor can be expressed as [13]

$$G_{ji} = \left(N_j - \frac{g_j}{g_i}N_i\right)\frac{h}{\lambda_{ji}}B_{ji}\Gamma(\nu) \tag{7}$$

where N_j and N_i are the populations of the upper and lower levels, respectively. For the laser transition, g_j is the degeneracy of energy level j; λ_{ji} is the laser transition wavelength; B_{ji} is the stimulated radiation coefficient; and $\Gamma(\nu)$ is the normalized line shape function.

The gain G can also be used to express the ease with which a population-inverted system undergoes ASE [14]. In this work, at the very beginning of each pumping pulse, levels $8^2P_{3/2}$ and $7^2P_{3/2}$ are empty, whereas the $7^2D_{5/2}$ is populated via two-photon excitation using the pumping laser. Therefore, population inversions form between the $7^2D_{5/2}$ and $8^2P_{3/2}$ states, and between the $7^2D_{5/2}$ and $7^2P_{3/2}$ states. Furthermore, the pumping area for this system is a thin and long pole-like area, which suits ASEs [15, 16]. As a result, ASEs of 2.42 and 36 μm are generated and the FWMs described in Eqs. (5) and (6) proceed, producing the UV and BLUE beams.

In Figs. 2 and 4, the generation of UV is seen to be more efficient than that of BLUE, as measured by either energy efficiency or quantum efficiency. The higher efficiency of UV is believed to result from a combination of both the high efficiency in generating the ASE beam of 36 μm and the high efficiency of the FWM process involving the 767.2 nm beam and the 36 μm ASE beam. Nevertheless, the contributions of ASE and FWM processes to UV generation were not distinguished because of the lack of data on the absolute intensities of the ASE beams at 2.42 and 36 μm.

However, when the laser beam is modulated, the ASE mechanism is changed. The modulated beam has the same wavelength as the transition $7^2D_{5/2} \rightarrow 7^2P_{3/2}$; as a result, this modulation serves as "seed light," which amplifies itself by diminishing much of the population in the $7^2D_{5/2}$ state. Thus, the population inversion of $7^2D_{5/2} \rightarrow 8^2P_{3/2}$ reduces considerably accompanied by a reduction in $G(7^2D_{5/2} \rightarrow 8^2P_{3/2})$ in accord with Eq. (7). Both ASE of 36 μm and UV are significantly weakened. The UV beam can only resurge if the modulated laser beam weakens. This result is quite consistent with pulse shapes (Fig. 8). The FWM of the pumping laser and the modulated laser beam produce a much larger BLUE energy beam than that without modulation. The situation here is similar to the 2.9-μm mid-infrared parametric up-conversion in Cs vapor [17].

Modulation of the output frequency or intensity in frequency up-conversions has been described in various works. For example, Akulshin et al. [18] report the conversion in Rb vapor of the dual-wavelength beams (780 and 776 nm) into 420 nm. With another counter-propagating beam at 795 nm, modulation of the intensity of the 420-nm beam was realized by varying the number density of Rb atoms on $5^2S_{1/2}$ ($F = 3$). Brekke et al. [19] report the conversion in Rb vapor of a 778-nm beam into 420 nm. The frequency of the 420-nm beam was modulated over a range of ~1 GHz by detuning the 778-nm beam. The energy levels related to both conversions mentioned above are shown in Fig. 3b.

The mechanisms involved in both systems studied by Akulshin et al. and Brekke et al. are related to the selection of the group with certain velocity of the Doppler-broadened Rb atoms resonating with the narrow-linewidth laser beams. The modulation mechanism of our system is different. No resolution of the different group velocities of the atoms is needed. The modulation is realized by changing the balanced ratio between the generation of ASEs at 2.4 and 36 μm.

3.3.3 Conversion efficiency

The energy conversion efficiency is moderate for our system. When Cs metal is heated to 200 °C, the vaporized Cs atom density is approximately 1×10^{15} cm^{-3}. The absorption linewidth is mainly determined by Doppler broadening; its full width at half maximum (FWHM) is [13]

$$\Delta\nu_{\text{Doppler}} = 2\nu_0\sqrt{\frac{2kT}{mc^2}\cdot \ln 2} \tag{8}$$

where ν_0 is the central absorption frequency, k Boltzmann's constant, T the absolute temperature, c the velocity of light, and m the mass of the Cs atom. $\Delta\nu(7^2D_{5/2})$ at 200 °C is calculated to be 1.0 GHz. The linewidth of the dye laser is approximately 3 GHz; however, the experimental tuning range is approximately 50 GHz (±0.05 nm). This result is a consequence of the high pumping power and nonlinear two-photon absorption by the Cs atoms, so the "wavelength wing tips" of the pumping laser beam can also be absorbed during up-conversion.

With modulation, the range of frequency tuning for the BLUE beam is as large as ~40 cm^{-1} (1.2 THz, detectable full range); see Fig. 6. This large range is related to the two different ways of generating BLUE. At the resonating wavelengths (Fig. 3a), the BLUE can be generated by ASE.

Also, if the modulated beam is far from the resonating wavelengths, BLUE is generated mainly through non-resonating FWM that occurs between the 778.1-nm pumping laser beam and the modulated beam (according to Eq. 1), and is believed to be generated without a participating ASE.

Figure 4 implies that the frequency up-conversion system is far from saturation. An absorption test indicates only a small amount of the pump laser is absorbed. The low efficiency can be attributed to the low two-photon absorption efficiency of $7^2D_{5/2}$ because the broad linewidth of the dye laser does not match up with the narrow linewidth of the atom absorption line [20].

The modulation can be viewed as a probe to prove the mechanism including ASE and FWM in the frequency up-conversion. The atomic energy level system is similar to other systems mentioned in the introduction. Trends encountered in this study are also expected to be applicable to those systems. Also, the results may be useful in improving the conversion efficiency of the system [4–9]. For example, we can expect to improve the efficiency of the process described by Eqs. (2)–(4) and Fig. 3b in Rb vapor using a 5.23-μm modulation laser.

4 Conclusion

Frequency up-conversion was demonstrated in Cs vapor. New wavelengths of 455.6 and 387.7 nm were obtained. The energy conversion efficiency was measured to be 0.03 and 0.08 %, respectively, and the output energies of the up-conversion show linear rise with increasing pumping power. Nanosecond-scale modulations of the frequency up-conversion were realized, and the wavelength of the BLUE beam can be precisely adjusted by fine-tuning the wavelength of modulation laser. Introducing a modulation laser enhances the intensity of the BLUE beam and suppresses the intensity of UV. Pulses of the output radiations occur simultaneously with the pump laser, while the addition of the modulation laser delays the generation of UV by 1.4 ns. Experimental results have proved that the mechanism of frequency up-conversion involves both ASEs and FWM together. This frequency up-conversion mechanism is expected to be applicable to other alkali–metal systems, and the efficiency of up-conversion can be improved by resonant excitation of Cs by a two-color two-photon process and narrower linewidths of the excitation lasers and modulation laser.

Acknowledgments This work is supported by the National Natural Science Foundation of China (Grant Nos. 61405197, 11304311, 11475177, and 61505210).

References

1. W. Pegau, D. Gray, J. Zaneveld, Appl. Optics **36**, 6035 (1997)
2. T. Narahara, S. Kobayashi, M. Hattori, Y. Shimpuku, G. Enden, J. Kahlman, M. Dijk, R. Woudenberg, Jpn. J. Appl. Phys. **39**, 912 (2000)
3. W. Krupke, Prog. Quant. Electron. **36**, 4 (2012)
4. A. Zibrov, M. Lukin, L. Hollberg, M. Scully, Phys. Rev. A **65**, 051801 (2002)
5. T. Meijer, J. White, B. Smeets, M. Jeppesen, R. Scholten, Opt. Lett. **31**, 1002 (2006)
6. J. Sell, M. Gearba, B. Depaola, R. Knize, Opt. Lett. **39**, 528 (2014)
7. A. Vernier, S. Franke-Arnold, E. Riis, A. Arnold, Opt. Express **18**, 17020 (2010)
8. G. Walker, A. Arnold, S. Franke-Arnold, Phys. Rev. Lett. **108**, 3533 (2012)
9. C. Sulham, G. Pitz, G. Perram, Appl. Phys. B **101**, 57 (2010)
10. J. Schultz, S. Abend, D. Döring, J. Debs, P. Altin, J. White, N. Robins, J. Close, Opt. Lett. **34**, 2321 (2009)
11. A. Akulshin, D. Budker, R. McLean, Opt. Lett. **39**, 845 (2014)
12. A. Smith, J. Ward, IEEE J. Quantum Electron. **17**, 525 (1981)
13. O. Svelto: Principles of Lasers (Fifth edition, Springer International Publishing AG1, 1998)
14. I. Okuda, T. Tomie, Y. Owadano, Appl. Phys. B **70**, 737 (2000)
15. L. Allen, G. Peters, Phys. Rev. A **8**, 2031 (1973)
16. B. Guzelturk, Y. Kelestemur, M. Olutas, S. Delikanli, H. Demir, ACS Nano **8**, 6599 (2014)
17. E. Stappaerts, S. Harris, J. Young, Appl. Phys. Lett. **29**, 669 (1976)
18. A.M. Akulshin, A.A. Orel, R.J. McLean, J. Phys. B **45**, 015401 (2012)
19. E. Brekke, E. Herman, Opt. Lett. **40**, 5674 (2015)
20. N. Georgiades, E. Polzik, H. Kimble, Opt. Lett. **19**, 1474 (1994)